JES, Vol. 54, No. 1, Jan. 2026 DOI: 10.21608/JESAUN.2025.364423.1437 Part D: Mining and Metallurgical Engineering

Journal of
Engineering Sciences
Faculty of Engineering
Assiut University

JES

مجلة
العلوم الهندسية
كلية الهندسة
جامعة أسيوط

journal homepage: http://jesaun.journals.ekb.eg

Comparative Analysis of Flux-Cored Arc Welding and Shielded Metal Arc Welding Processes on Hardox 450 Steel: Microstructural, Mechanical, and Fractographic Investigation

Received 3 May 2025; Revised 14 August 2025; Accepted 14 August 2025

Mohamed M. Terra [1]
Mohamed M. El-sayed Seleman [2]
Mohamed I.A. Habba[3]

Keywords
Hardox 450; FCAW; SMAW; Mechanical Properties; Microstructure.

Abstract: This study investigates the microstructural and mechanical properties of Hardox 450 steel joints welded using flux-cored arc welding (FCAW) and shielded metal arc welding (SMAW) techniques. Hardox 450 steel plates with a thickness of 4 mm were welded using AWS A5.20 E71T-1C filler rods for FCAW and AWS A5.1 E7018 filler rods for SMAW. The welded joints were characterized through macrostructural and microstructural examinations using optical microscopy and scanning electron microscopy (SEM), as well as Rockwell hardness tests and tensile property evaluations. The results showed that both FCAW and SMAW produced defect-free welds with acceptable reinforcement heights and well-defined fusion zones, heat-affected zones (HAZ), and weld zones (WZ). The hardness measurements revealed lower hardness values in the WZ compared to the HAZ and base metal for both welding processes, with FCAW joints exhibiting higher WZ hardness than SMAW joints. Tensile tests demonstrated that the FCAW joints had superior tensile strength of 903.8 MPa compared to the SMAW joints of 755.6 MPa, representing joint efficiencies of 65% and 55%, respectively, relative to the base material of 1385.5 MPa). However, the SMAW joints displayed higher fracture strain of 17.1% than the FCAW joints of 13.6%, indicating greater ductility. Fracture surface analysis using SEM revealed distinct failure mechanisms, with the FCAW joints exhibiting more pronounced cleavage facets and brittle fracture characteristics compared to the SMAW joints. The findings highlight the influence of welding processes and filler materials on the microstructure and mechanical properties of Hardox 450 steel weldments.

1. Introduction

Hardox Steel is an abrasion-resistant steel developed by SSAB, a Swedish steel manufacturer. They have high hardness and toughness, making them well suited for applications with severe wear and

[1] MSc student., Department of Metallurgical and Materials Engineering, Faculty of Petroleum and Mining Engineering, Suez University, Suez 43221, Egypt, mohamed.mote@pme.suezuni.edu.eg
[2] Professor of Metallurgical and Materials Engineering, Department of Metallurgical and Materials Engineering, Faculty of Petroleum and Mining Engineering, Suez University, Suez 43221, Egypt, mohamed.elnagar@suezuniv.edu.eg
[3] Asst. Professor, Mechanical (Production) Department- Faculty Technology & Education, Suez University, Suez 43221, Egypt, mohamed.atia@suezuniv.edu.eg

https://doi.org/10.21608/jesaun.2025.364423.1437

impact [1,2]. Hardox steels achieve their desired properties by alloying elements such as chromium, molybdenum, and boron, as well as by specialized heat treatment and processing methods [3]. They are commonly used in mining and construction equipment, truck bodies, agricultural machinery, and other applications where durability against abrasion and impact are critical. Hardox steels encompass a range of grades, including Hardox 400, Hardox 450, Hardox-500, and Hardox-600, based on the Brinell hardness of Hardox steel [4,5]. Different grades of Hardox steel offer a range of wear resistance and toughness levels to suit different needs. Hardox 450 is a high-strength abrasion-resistant steel composed primarily of iron, carbon, manganese, and trace amounts of other elements, such as chromium, nickel, and molybdenum [6]. Its advantage over traditional steel alloys [7,8] is its exceptional hardness, toughness, and wear resistance, which make it ideal for applications that require extreme durability [9]. These properties of Hardox 450 (minimum tensile strength of approximately 1400 MPa and Rockwell hardness of 450 HRC) make it suitable for many heavy and harsh industrial applications such as construction, mining, agriculture, and manufacturing of components such as buckets, liners, and cutting edges, as it can withstand harsh conditions, resist abrasion, and prolong the lifespan of equipment subjected to heavy wear and tear [9,10]. For the aforementioned Hardox 450 applications, welding is necessary to fabricate components or structures using Hardox 450 steel, particularly in the mining, construction, and manufacturing industries. However, welding Hardox 450 can be challenging because of its hardness and susceptibility to cracking [11,12]. Therefore, the welding of Hardox steel should carefully consider the applied techniques, as well as the preheating and post-weld heat treatment, to ensure high-quality weldments. The selection of welding techniques that preserve the hardness and toughness of Hardox steel is critical [13–15]. Despite the wide range of uses of Hardox steels and the necessity of welding these steels into various grades, less research has been conducted on the welding of Hardox steel grades. **Table 1** presents previous studies that have focused on welding different grades of Hardox steel grades using different parameters, such as filler materials and post-heat treatment, using different welding methods.

Table 1. Previous studies have focused on welding different grades of Hardox steel.

No.	Authors	Hardox Steel	Welding process	Parameters	General observations
1-	Gupta et al. [16]	400	SMAW	Filler materials: E8018, E9018 and E11018	The highest hardness of WZ attains 52% of initial steel plate (E11018), the highest join efficiency 57% (E11018), and the highest yield strength 63% (E9018)
2-	Konat et al. [17]	450	SAW	Post-weld heat treatment	The thermal heat treatment increases the joint strength of the weld zone from 50% to 85% of the initial steel plate.
3-	Frydman et al. [3]	400 and 500	SAW	Post-weld heat treatment	The results showed a 50% reduction in hardness of WZ for both steels. After heat treatment, significant improvement reaches 70% for Hardox 400 and 90% for Hardox 500 steel compared to initial steel plate.
4-	Konat [18]	600	SAW	Post-Weld Heat Treatment	Improvement in weld zone hardness and tensile strength of the heat-treated joints compared to the non-treated joints.
5-	Mazur et al. [11]	450	GMAW	Welding wire diameter	Hardness profiles are identical for both diameters of the fillers used for welding and approximate 50% of initial steel plate

No.	Authors	Hardox Steel	Welding process	Parameters	General observations
6-	Baskutis et al. [19]	450	TIG	Filler materials and additives	The additives stabilize retained austenite, preventing it from transforming into martensite during welding and improving joint strength and flexibility.

Based on existing literature, the necessity of joining Hardox steel for various engineering applications is underscored by current research, which also reveals inconsistencies in fusion welding outcomes for Hardox 450 steel and a lack of established methods for thin sections. These knowledge gaps necessitate further studies. Therefore, thorough research into different welding techniques for joining Hardox 450 steel, particularly in thin thicknesses, is required, along with comparative analyses to understand their impact on joint performance. In response to these needs, this study presents a comparative investigation of FCAW and SMAW welding processes on the quality of welds in 4 mm thick Hardox 450 steel.

The influence of various welding procedures and their associated parameters on the overall quality of welded joints was investigated through a comprehensive analysis involving macrostructural and microstructural (optical microscopy; OM and scanning electron microscopy; SEM) examinations, hardness tests, and tensile tests. Rockwell hardness measurements were conducted at the mid-thickness of cross-sections in a linear direction perpendicular to the weld path using hardness Rockwell scale "A" with 2 mm interval spacing between measurements. Tensile testing was performed using universal testing equipment following ASTM-E8 subsize specimen dimensions to evaluate the mechanical properties and joint efficiency of the welded joints. Additionally, fracture analysis of the tensile-tested specimens of Hardox 450 steel weldments was performed using SEM to investigate the failure mechanisms and microstructural characteristics of the fracture surfaces.

2. Experimental Procedure

2.1. Initial steel plates

Hardox 450 steel plates were welded in a butt joint design using two welding methods: FCAW and SMAW. The Initial steel plates were Hardox 450 steel received without any additional heat treatment with dimensions of 100 × 150 × 4 mm, which was supplied by the BSF-Egypt company, Alexandria, Egypt. The Hardox 450 steel plates were delivered with an as-rolled surface and mill edge finish. The chemical composition of Hardox 450 steel plates is primarily composed of iron, with significant alloying elements such as carbon (0.26 wt.%), manganese (1.60 wt.%), and silicon (0.70 wt.%), chromium (1.40 wt.%), nickel (1.50 wt.%), molybdenum (0.60 wt.%), boron (0.005 wt.%), phosphorus (0.025 wt.%), and sulfur (0.010 wt.%). The carbon equivalent value (CEV) ranges between 0.39 and 0.48, which is a crucial metric for understanding the weldability of the material. Before implementing the welding techniques (FCAW and SMAW), thorough mechanical and chemical cleaning procedures were conducted on the edges of the Hardox plates. This cleaning process aims to eradicate potential sources of contamination, including dust, rust, moisture, and oil. The objective was to prevent the infiltration of these contaminants into the weld zone, because their presence could lead to welding defects.

2.2. Welding of Hardox 450 steel plates

The 4 mm thick Hardox 450 steel plates were machined to receive a Single V-groove with a 60° angle and a 2 mm root face for both welding techniques. **Figure 1** illustrates the joint design applied to both welding processes (all dimensions in mm). The groove geometry was carefully controlled to ensure consistent weld penetration and joint quality across both FCAW and SMAW processes."

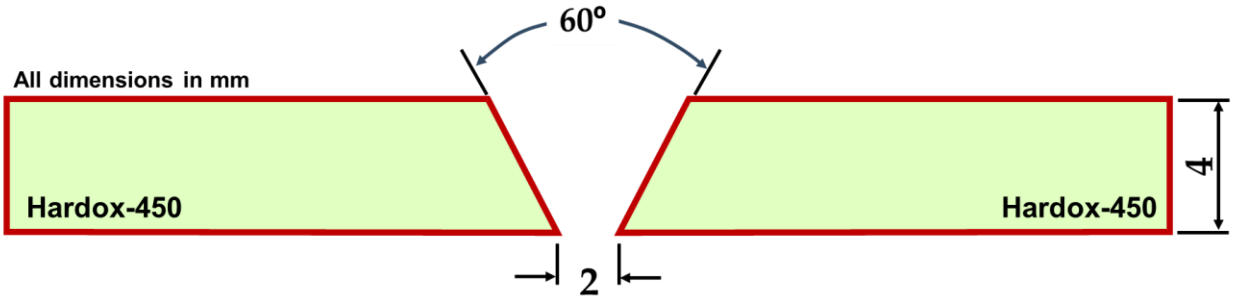

Figure 1. Schematic illustration of the single V-groove joint design employed for both the FCAW and SMAW welding processes (All dimensions in mm).

For the FCAW welding method, the weldments of Hardox 450 joints were conducted using the FCAW welding machine model Powertech 505S (LINCOLN ELECTRIC Co., CLEVELAND, USA) using 2.5 mm diameter filler rods of AWS a5.1 E7018, Telwin, China. The SMAW welding machine model R3R 600-I (LINCOLN ELECTRIC Co., CLEVELAND, USA) welding machine was utilized for the SMAW of Hardox 450 steel using 1.5 mm diameter AWS A5.20 E71T-1C filler rods (Xiang Welding Industrial Co Ltd, Tianjin, China). Two different filler rods were utilized for the welding of Hardox 450 steel using two methods: FCAW and SMAW. The FCAW method employs E7018 filler rods, composed of 0.07% carbon, 0.61% silicon, 0.87 wt.% manganese, and trace amounts of phosphorus (0.015wt.%), sulfur (0.011 wt.%), nickel (0.02 wt.%), chromium (0.03 wt.%), vanadium (0.01 wt.%), and molybdenum (0.01%). In contrast, the SMAW method uses E71T-1C filler rods, with a composition of 0.04 wt.% carbon, 0.55 wt.% silicon, 1.25 wt.% manganese, and similar trace levels of phosphorus (0.015 wt.%) and sulfur (0.012 wt.%). The welding parameters for the FCAW and SMAW methods used on Hardox 450 steel. Both methods utilized a single V-groove joint design and required two passes for welding. The FCAW process employed AWS A5.20 E71T-1C filler rods and operated with a current range of 200–280A and DC+ polarity. In contrast, the SMAW process used AWS A5.1 E7018 filler rods with a lower current range of 110–145A and the same DC+ polarity, as lists in **Table 2**.

Table 2. Welding Parameters for Butt-Welding 4 mm-thick Hardox 450 Steel using FCAW and SMAW.

Parameter	FCAW	SMAW
Current range (A)	200-280	110-145
Voltage (V)	26-30	22-26
Filler material	AWS A5.20 E71T-1C	AWS A5.1 E7018
Filler diameter (mm)	1.5	2.5
Travel speed (mm/min)	150-180	120-150

2.3. Characterization of Hardox 450 weldments

The weldments made from Hardox 450 steel were examined through macrostructure and microstructure (using both OM and SEM). Rockwell hardness and tensile tests were also performed to assess the impact of the FCAW and SMAW processes on the quality and efficiency of 4 mm thick

Hardox 450 steel weldments. A wire-cutting machine (V400G Plus, Excetek Technologies Co., Taichung, Taiwan) was employed to extract the test samples for metallographic analysis, hardness, and tensile evaluation of the welded Hardox 450 steel joints. Cross-sections of the welded specimens were prepared for metallographic analysis by grinding them with emery paper up to a grit size of 2500. Subsequently, a polishing step was performed using a 0.5 µm Al_2O_3 paste. Finally, the specimens underwent an etching process utilizing Nital Etchant (4 % Nitric Acid) for 4 s. The Rockwell hardness (Rockwell Hardness Tester, DM-XHRD150, Osaka, Japan) test was conducted on the Hardox 450 steel weldments at the mid-thickness of the cross-section, in a predetermined linear direction perpendicular to the weld path, as shown in Figure 2. All measurement locations and spacing intervals shown in Figure 2 are in mm. The hardness measurements were conducted using a Rockwell hardness tester using the hardness Rockwell scale "A" with 2 mm interval spacing between each measurement. The tensile test for the Hardox 450 weldments was performed using universal testing equipment (WDW-300D Testing equipment, Guangdong, China). The dimensions of the tensile test sample, as per the ASTM-E8 subsize, are illustrated in Figure 3. The fracture surfaces of the tensile specimens were examined using scanning electron microscopy (SEM; Quanta FEG 250SFEI Company, Hillsboro, OR, USA).

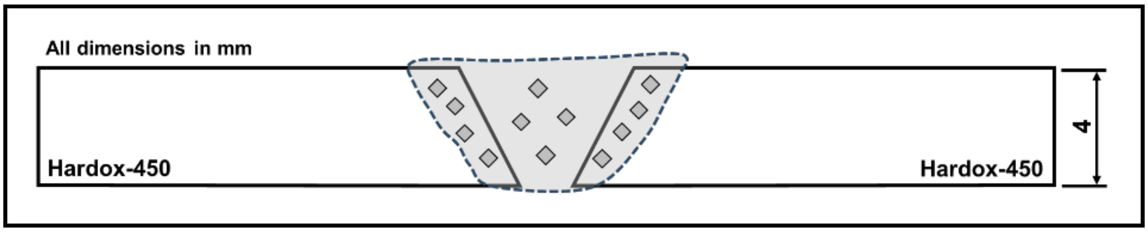

Figure 2. Hardness measurement's location of the SMAW and FCAW welded joints (All dimensions in mm).

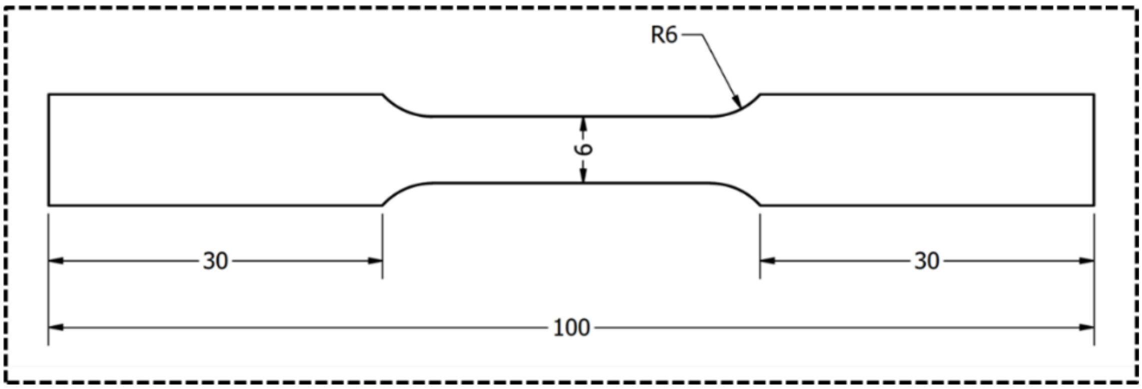

Figure 3. Dimensions of the extracted tensile test specimens (ASTM E8, All dimensions in mm).

3. Results and discussions

3.1. Macro and microstructure analysis

Figures 4 and 5 show the visual photo and macrostructure of the SMAW and FCAW welded joints, respectively. According to the visual photos of welded joints, both methods produced defect-free welds with acceptable reinforcement heights ranging from 2.0 to 2.8 mm, depending on the process. Specifically, the path width of the SMAW joints ranged from 10–11 mm (Figure 4 a and b), while the FCAW joints exhibited slightly narrower paths of 9–10 mm (Figure 5 a and b). These results indicate that the selected welding techniques and filler rods (AWS A5.1 E7018 for SMAW and AWS A5.20 E71T-1C for FCAW) are suitable for fabricating Hardox 450 joints, ensuring sound weld quality without visible surface anomalies. Macrostructural analysis provided deeper insights into the integrity and quality of the welded joints. Cross-sectional examinations of the 4 mm thick Hardox 450 weldments revealed well-defined fusion zones, heat-affected zones (HAZ), and weld zones (WZ) for both SMAW (Figure 4c) and FCAW (Figure 5c) processes. The transition between the HAZ and WZ was smooth, and no internal defects such as cracks, voids, or incomplete fusion were observed. The macrographs showed complete penetration and uniform joint formation, which underscores the efficacy of the applied welding parameters and filler materials. Additionally, the filler rods used in both processes contributed to the structural soundness of the welds. These findings confirm that the SMAW and FCAW methods are both capable of producing sound weldments in Hardox 450 steel.

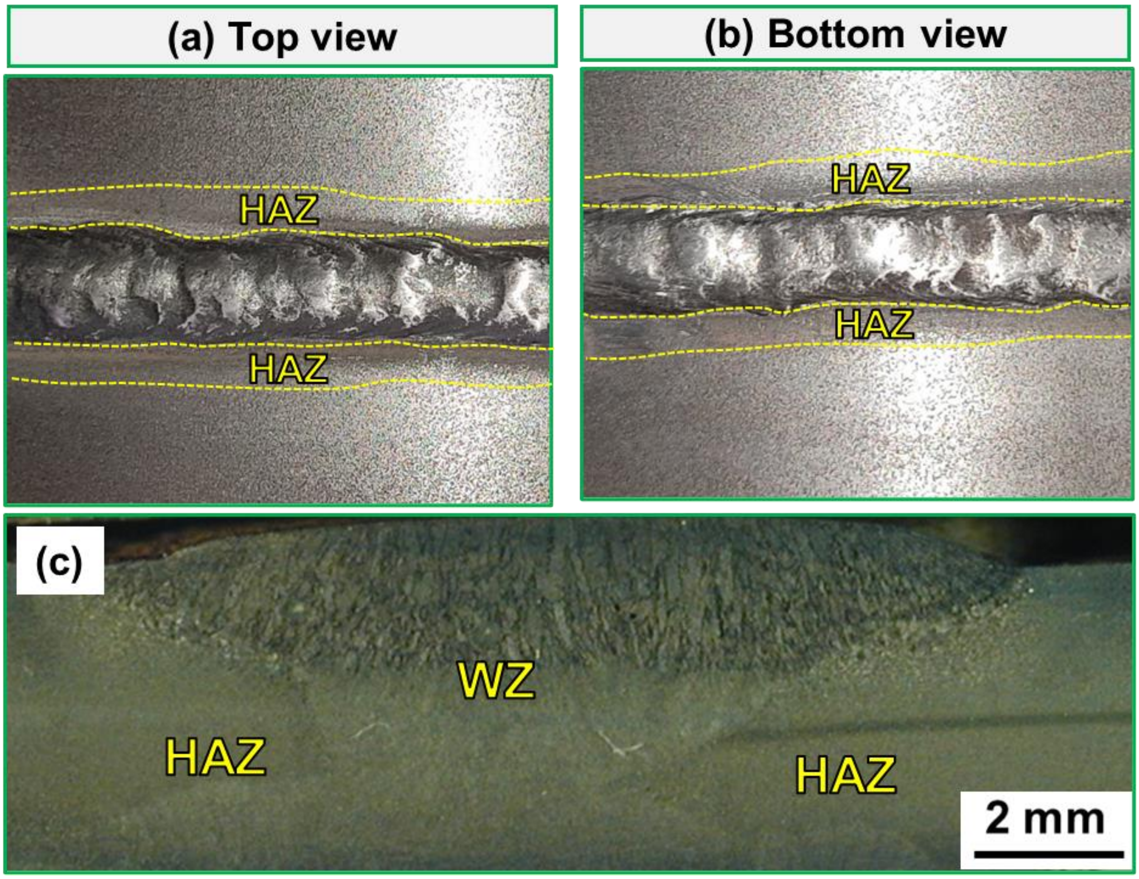

Figure 4. SMAW welded Hardox 450 steel joints: (a) top view, (b) bottom view, and (c) cross-sectional macrostructure.

.

3.2. Mechanical properties

The hardness properties of the Hardox 450 steel welded joints were systematically evaluated to assess the effects of the SMAW and FCAW processes on the WZ, HAZ, and base material, as shown in Figure 7. The results indicate significant variations in hardness profiles across the welded joints, attributable to differences in thermal cycles, filler materials, and welding parameters. The hardness measurements revealed that the WZ of both SMAW and FCAW joints exhibited lower hardness values compared to the HAZ and base metal (Figure 7). This reduction is attributed to the rapid cooling rates and solidification processes during welding, which result in localized segregation of alloying elements in the WZ. Specifically, the WZ hardness values peaked at 58.5 HRA for SMAW joints and 64.5 HRA for FCAW joints, as shown in Figure 7. These values were consistently lower than the corresponding HAZ and base metal, demonstrating that the welding processes altered the microstructural features of the WZ, reducing its hardness. The FCAW process yielded a higher WZ hardness compared to SMAW, which can be explained by its higher amperage range (200–280 A) and the higher manganese content in the E71T-1C filler rod. Manganese plays a crucial role in promoting acicular ferrite formation, a microstructural feature known for its high toughness and resistance to crack propagation [16,20]. Additionally, the improved fusion achieved at higher amperage settings minimizes defects such as porosity and slag inclusions, further contributing to the higher hardness values observed in FCAW joints [16,20]. On the other hand, the SMAW process, operating at a lower amperage range (110–145 A) with the E7018 filler rod, resulted in comparatively lower hardness in the WZ. While the lower heat input in SMAW helps to control the thermal impact on the HAZ, it may also limit the extent of alloying element diffusion, leading to reduced hardness in the weld zone. The HAZ exhibited higher hardness than the WZ in both welding processes (65.8 for SMAW and 86.1 for FCAW), reflecting the localized thermal effects of welding. The HAZ's proximity to the fusion line leads to rapid heating and cooling, which promotes the formation of martensitic or bainitic microstructures, characterized by higher hardness.

This hardness gradient across the joint underscores the importance of controlling welding parameters to prevent excessive brittleness in the HAZ, which could compromise the joint's overall mechanical performance. LAZIĆ et al. [12] investigated the Hardox 450 steel for manufacturing welded assemblies in the military industry. It analyzes the weldability of this steel and prescribes an appropriate welding technology, including the selection of filler metal, welding parameters, and preheating temperatures. The experimental section focuses on hardness testing and microstructural analysis of the welded joint zones. Hardness testing revealed that the maximum hardness values in the HAZ and weld metal were significantly lower than those in the base metal.

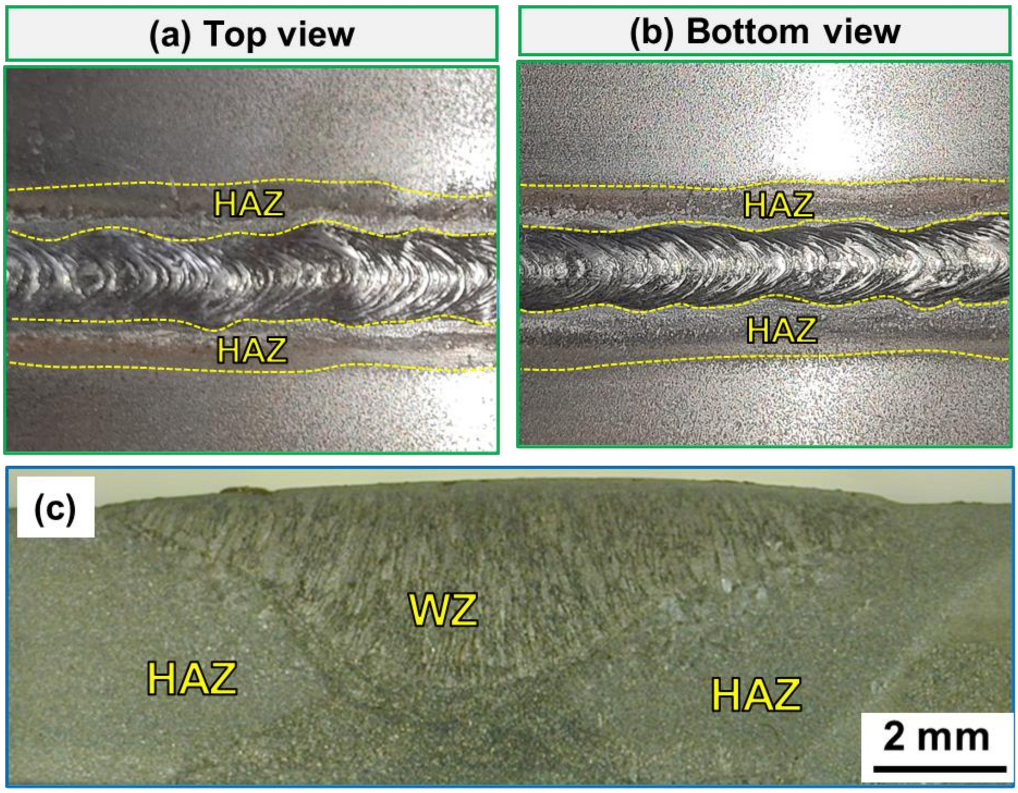

Figure 5. FCAW welded Hardox 450 steel joints: (a) top view, (b) bottom view, and (c) cross-sectional macrostructure.

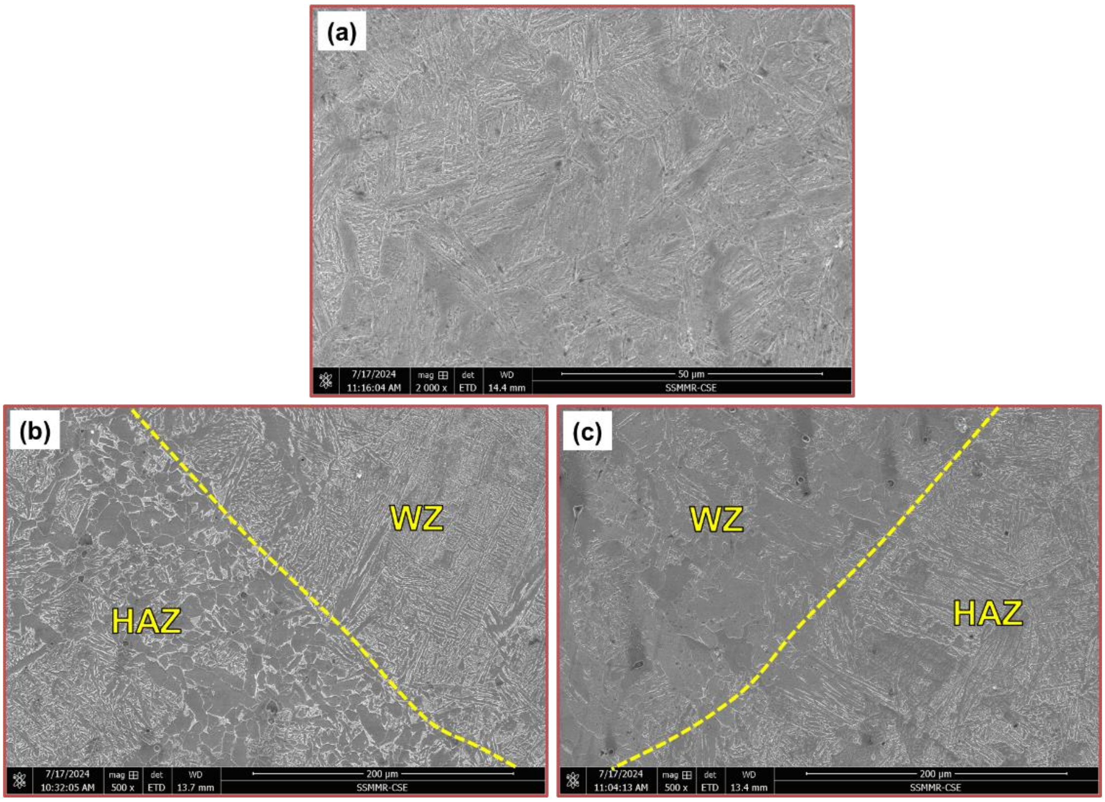

Figure 6. Microstructure of the (a) Hardox 450 initial plate, (b) SMAW Welded joint, (c) FCAW welded joint.

Despite avoiding the formation of brittle martensite, undesirable decreases in hardness and strength occurred in the HAZ and weld metal regions. This decrease in hardness was attributed to uneven heating and cooling cycles during welding. The lower hardness area in the HAZ was identified as a potentially critical region that is susceptible to fracture, particularly under tensile and fatigue conditions. Zuo et al. [21] investigated the properties of Hardox-500 steel TIG-welded joints using different filler weld wires. They found that the hardness of the WZ decreased compared to that of the HAZ and the initial steel plate. Furthermore, the choice of filler weld wire significantly influenced the hardness of the Hardox 500 steel TIG-welded joints. Welding metals obtained using high-strength filler wires, such as ER110S-G and E110C-G, exhibit higher hardness values than those welded with conventional solid wires, such as ER70S-6. The increased hardness of the weld metals realized with high-strength filler wires was attributed to their higher alloy content and finer microstructural features, consisting of low-carbon martensitic laths and retained austenite.

Table 3 summarizes the tensile results of the initial plate and SMAW and FCAW welded joints. It can be remarked that the tensile properties of the Hardox 450 base material and its welded joints, produced by SMAW and FCAW, reveal significant differences influenced by the welding processes and filler materials. The base material exhibited a tensile strength of 1385.5 MPa and an elongation of 11.8%, reflecting its high strength and moderate ductility due to its martensitic microstructure. In comparison, the tensile strength of the SMAW and FCAW welded joints was reduced to 755.6 MPa and 903.8 MPa, respectively, representing joint efficiencies of 55% and 65%. This reduction is primarily attributed to the thermal cycles during welding, which alter the microstructure in the WZ and HAZ, leading to softer and coarser phases, such as ferrite and bainite, compared to the base metal's martensite [10,22]. The FCAW joints demonstrated superior tensile strength compared to SMAW joints, which can be attributed to the higher manganese content in the E71T-1C filler rod and the higher amperage range (200–280 A) used in the process. These factors promote better fusion, reduced defects, and the formation of acicular ferrite in the WZ, enhancing toughness and strength [23]. Conversely, SMAW joints, welded with E7018 filler rods and a lower amperage range (110–145 A), exhibited lower tensile strength, reflecting less effective fusion and the formation of a less refined microstructure in the WZ. In terms of ductility, the SMAW joints displayed a higher fracture strain of 17.1% compared to the FCAW joints' 13.6%, indicating greater elongation before failure. This enhanced ductility in SMAW joints suggests a trade-off between strength and flexibility, potentially making them more suitable for applications requiring deformation tolerance.

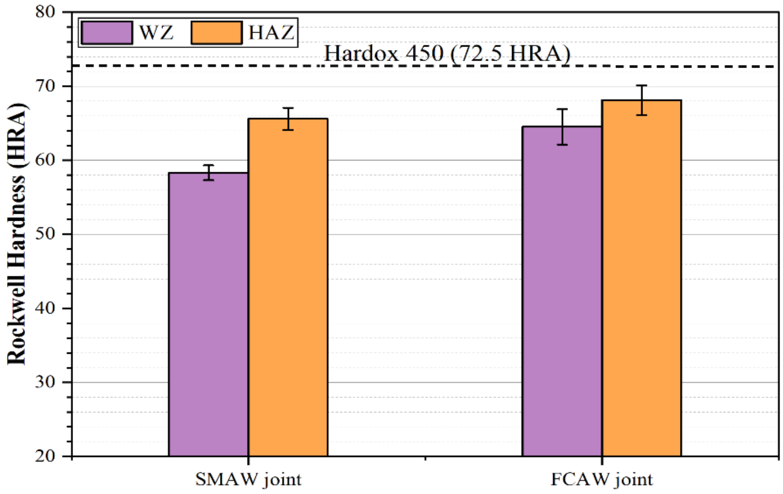

Figure 7. WZ, HZA, and BM Hardness measurements of the FCAW and SMAW welded joints.

Table 3. Tensile results of the Hardox 450 Initial plate, SMAW, and FCAW welded joints

Material	Ultimate Tensile Strength (UTS) (MPa)	Fracture strain (%)	Joint efficiency (%)
Hardox 450	1385.5	11.8	-
SMAW Joint	755.6	17.1	55
FCAW Joint	903.8	13.6	65

Konat et al. [17] examined the effects of post-weld heat treatment on the tensile properties of Hardox 450 steel welded joints. They used the SMAW process and found that thermal heat treatment significantly increased the joint strength from 50% to 85% of the strength of the initial steel plate. This improvement highlights the effectiveness of post-weld heat treatment in enhancing the mechanical properties of the weld zone, which is crucial for maintaining the structural integrity of welded joints in high-strength steels. Zuo et al. [21] focused on the tensile properties and microstructural characteristics of Hardox 500 steel joints welded using TIG welding with different filler weld wires. They highlighted the significant impact of filler wire selection on the mechanical properties of welded joints. Specifically, the study found that using high-strength filler wires, such as ER110S-G and E110C-G, resulted in weld metals with higher hardness and tensile strength than those welded with conventional solid wires, such as ER70S-6. The enhanced mechanical properties were attributed to the higher alloy content and finer microstructural features, including low-carbon martensitic laths and retained austenite, present in the WZ when high-strength fillers were used. Furthermore, when comparing the tensile properties of the welded joints with those of the initial steel plate, it was observed that the hardness of the WZ was lower than that of the initial steel plate. In this study, the initial Hardox 450 plate exhibited a tensile strength of 1385.5 MPa and a fracture strain of

11.8%. With respect to the Hardox 450 plate, the tensile strength ratios for SMAW and FCAW are approximately 0.55 and 0.65, respectively, and the fracture toughness ratios are approximately 0.92 and 0.79 for SMAW and FCAW, respectively. These findings suggest that FCAW offers better tensile strength and joint efficiency, while SMAW provides greater ductility.

Figure 8 shows the fracture surfaces of the Hardox 450 base material and its welded joints produced using SMAW and FCAW. The fractography illustrates the distinct failure mechanisms and microstructural changes resulting from the welding processes. The fracture surface of the Hardox 450 base material (Figure 8a) exhibits a uniform and fine dimpled texture, characteristic of ductile failure. This is consistent with its high tensile strength of 1385.5 MPa and elongation of 11.8%, indicating a balanced combination of strength and ductility due to its martensitic microstructure. In contrast, the SMAW welded joint (Figure 8b) shows a fracture surface with mixed characteristics, indicating a combination of ductile and brittle failure modes. The presence of larger dimples alongside some cleavage facets suggests reduced ductility compared to the base material. This is corroborated by its lower tensile strength of 755.6 MPa and increased elongation of 17.1%, signifying a trade-off between strength and ductility. The fracture surface of the FCAW welded joint (Figure 8c) demonstrates more pronounced cleavage facets and a relatively coarser texture, indicating a predominance of brittle fracture mechanisms. This aligns with the higher tensile strength (903.8 MPa) and reduced elongation (13.6%) observed for FCAW joints, reflecting a stronger but less ductile weld. The higher manganese content in the E71T-1C filler rod and the higher amperage used in FCAW enhancing strength but at the expense of ductility. Wang et al. [24] investigated the fracture surface of the HARDOX450 steel after conducting the tensile test. They observed ductile dimples resulting from micro-void coalescence, tear ridges. In addition to, secondary cracks along various directions, and few cleavage facets. Moreover, secondary and delamination cracks are commonly observed in rolled steel sheets [25]. These results are in agreement with our fracture surface observations.

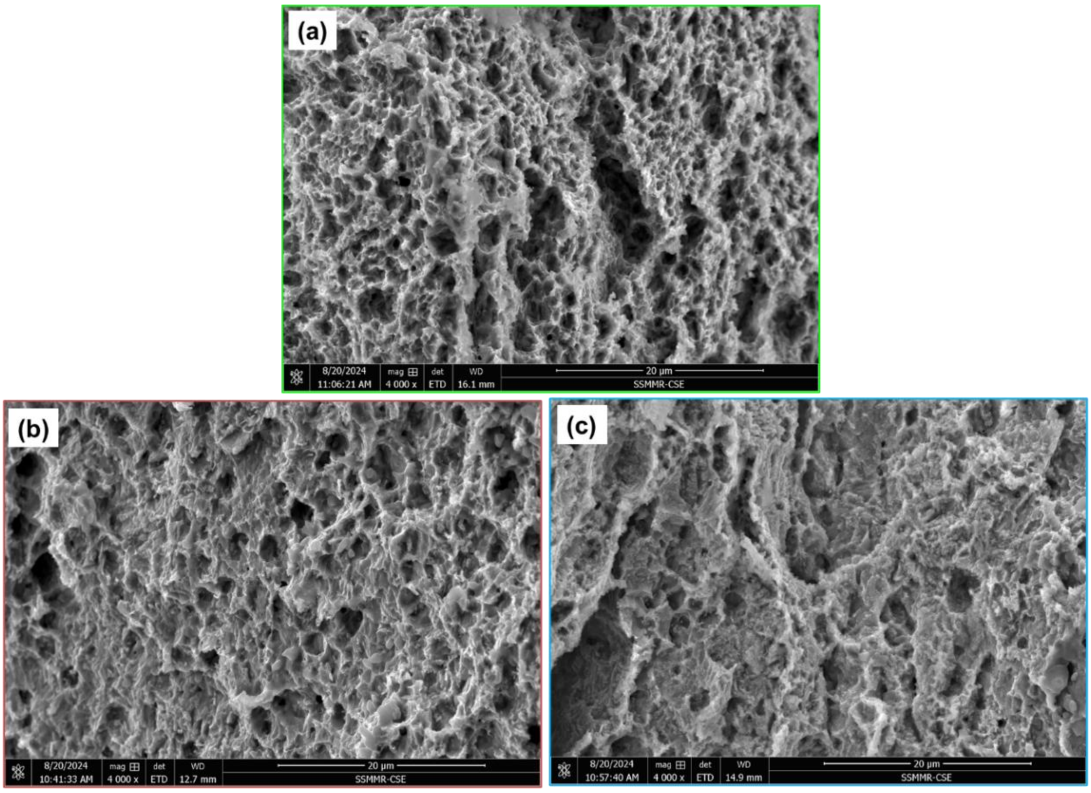

Figure 8. Fracture surface morphology of (a) base Hardox 450 steel plate, and welded joints using (b) SMAW and (c) FCAW processes.

4. Conclusions

This study aimed to compare the effects of SMAW and FCAW welding processes on the microstructure and mechanical properties of Hardox 450 steel joints. The key findings can be summarized as follows:

- Both SMAW and FCAW processes produced defect-free welds with acceptable overall quality, demonstrating their suitability for joining Hardox 450 steel.
- FCAW joints exhibited superior tensile strength (903.8 MPa) compared to SMAW joints (755.6 MPa), with joint efficiencies of 65% and 55% respectively, relative to the base material.
- SMAW joints displayed higher ductility with a fracture strain of 17.1% compared to 13.6% for FCAW joints.
- Hardness measurements revealed significant variations across the weld zones, with specific values demonstrating the influence of welding parameters on material properties. The base metal exhibited an average hardness of 445 ± 8 HRA, while the weld metal showed hardness values ranging from 420 to 435 HRA depending on the welding procedure employed. The heat-affected zone (HAZ) displayed the most notable variations, with hardness values decreasing to 380-410 HRA in the coarse-grained HAZ and recovering to 425-440 HRA in the fine-grained HAZ.
- Fracture surface analysis indicated distinct failure mechanisms, with FCAW joints exhibiting more pronounced cleavage facets and brittle fracture characteristics.

References

1. Turichin, G.; Tsibulskiy, I.; Kuznetsov, M.; Akhmetov, A.; Klimova-Korsmik, O. Hybrid Laser-Arc Welding Tanks Steels. *IOP Conf Ser Mater Sci Eng* **2016**, *125*, doi:10.1088/1757-899X/125/1/012002.
2. Rajput, V.; Goud, M.; Suri, N.M. *Performance Analysis of ECDM Process Using Surfactant Mixed Electrolyte*; 2020; Vol. Part F255; ISBN 9789811546181.
3. Frydman, S.; Konat; Pekalski, G. Structure and Hardness Changes in Welded Joints of Hardox Steels. *Archives of Civil and Mechanical Engineering* **2008**, *8*, 15–27, doi:10.1016/s1644-9665(12)60118-6.
4. Gallina, B.; Volcanoglo Biehl, L.; Braz Medeiros, J.L.; de Souza, J. The Influence of Different Heat Treatment Cycles on the Properties of the Steels HARDOX® 500 and STRENX® 700. *Revista Liberato* **2020**, 67–74, doi:10.31514/rliberato.2020v21n35.p67.
5. Konovalov, S. V.; Kormyshev, V.E.; Nevskii, S.A.; Ivanov, Y.F.; Gromov, V.E. Formation Wear Resistant Coatings on Martensite Steel Hardox 450 by Welding Methods. *IOP Conf Ser Mater Sci Eng* **2016**, *142*, doi:10.1088/1757-899X/142/1/012079.
6. BIAŁOBRZESKA, B.; KONAT, Ł. Comparative Analysis of Abrasive-Wear Resistance of Brinar and Hardox Steels. *Tribologia* **2018**, *272*, 7–16, doi:10.5604/01.3001.0010.6261.
7. Ahmed, M.S.I.; Ahmed, M.M.Z.; Abd El-Aziz, H.M.; Habba, M.I.A.; Ismael, A.F.; El-Sayed Seleman, M.M.; Abd El-Aty, A.; Alamry, A.; Alzahrani, B.; Touileb, K.; et al. Cladding of Carbon Steel with Stainless Steel Using Friction Stir Welding: Effect of Process Parameters on Microstructure and Mechanical Properties. *Crystals (Basel)* **2023**, *13*, doi:10.3390/cryst13111559.
8. Fouad, R.A.; Habba, M.I.A.; Elshaghoul, Y.G.Y.; Seleman, M.M.E.-S.; Hafez, K.M.; El-Fahhar, H.H.; Barakat, W.S. Comparative Analysis of Filler Metals on Microstructure and Mechanical Performance of TIG-Welded AISI 201 Austenitic Stainless-Steel Joints. *Science and Technology of Welding and Joining* **2024**, *29*, 356–367, doi:10.1177/13621718241283374.
9. Harinarayanan, G.; Krishnan, V.K.; Natarajan, M.P.; Surender, V.; Gowthaman, J. Wear Behavior and Wear Worn Surface Analysis on Hardox Steel. *Key Eng Mater* **2022**, *935*, 99–104, doi:10.4028/p-09akh6.
10. Kim, B.E.; Park, J.Y.; Lee, J.S.; Lee, J.I.; Kim, M.H. Effects of the Welding Process and Consumables on the Fracture Behavior of 9 Wt.% Nickel Steel. *Exp Tech* **2020**, *44*, 175–186, doi:10.1007/s40799-019-00321-3.

11. Mazur, M.; Ulewicz, R.; Bokůvka, O. The Impact of Welding Wire on the Mechanical Properties of Welded Joints. *Materials Engineering - Materiálové inžinierstvo* **2014**, *21*, 122–128.
12. Lazić, V.; Arsić, D.; Nikolić, R.R.; Djordjević, D.; Prokić-Cvetković, R.; Popović, O. Application of the High Strength Steel HARDOX 450 for Manufacturing of Assemblies in the Military Industry. *Key Eng Mater* **2017**, *755*, 96–105, doi:10.4028/www.scientific.net/KEM.755.96.
13. Fouad, R.A.; Habba, M.I.A.; Elshaghoul, Y.G.Y.; El-Sayed Seleman, M.M.; Hafez, K.M.; Hamid, F.S.; Barakat, W.S. The Influence of Various Welding Wires on Microstructure, and Mechanical Characteristics of AA7075 Al-Alloy Welded by TIG Process. *Sci Rep* **2024**, *14*, 19023, doi:10.1038/s41598-024-69227-4.
14. Elmas, M.; Koçar, O.; Anaç, N. Study of the Microstructure and Mechanical Property Relationships of Gas Metal Arc Welded Dissimilar Protection 600T, DP450 and S275JR Steel Joints. *Crystals 2024, Vol. 14, Page 477* **2024**, *14*, 477, doi:10.3390/CRYST14050477.
15. Habba, M.I.A.; Alsaleh, N.A.; Badran, T.E.; El-Sayed Seleman, M.M.; Ataya, S.; El-Nikhaily, A.E.; Abdul-Latif, A.; Ahmed, M.M.Z. Comparative Study of FSW, MIG, and TIG Welding of AA5083-H111 Based on the Evaluation of Welded Joints and Economic Aspect. *Materials* **2023**, *16*, doi:10.3390/ma16145124.
16. Gupta, A.; Sharma, V.; Kumar, P.; Thakur, A. Investigating the Effect of Ferritic Filler Materials on the Mechanical and Metallurgical Properties of Hardox 400 Steel Welded Joints. *Mater Today Proc* **2020**, *39*, 1640–1646, doi:10.1016/j.matpr.2020.05.788.
17. Konat, Ł.; Zemlik, M.; Jasiński, R.; Grygier, D. Austenite Grain Growth Analysis in a Welded Joint of High-Strength Martensitic Abrasion-Resistant Steel Hardox 450. *Materials* **2021**, *14*, doi:10.3390/ma14112850.
18. Konat, Ł. Technological, Microstructural and Strength Aspects of Welding and Post-Weld Heat Treatment of Martensitic, Wear-Resistant Hardox 600 Steel. *Materials* **2021**, *14*, doi:10.3390/ma14164541.
19. Baskutis, S.; Baskutiene, J.; Dragašius, E.; Kavaliauskiene, L.; Keršiene, N.; Kusyi, Y.; Stupnytskyy, V. Influence of Additives on the Mechanical Characteristics of Hardox 450 Steel Welds. *Materials* **2023**, *16*, doi:10.3390/ma16165593.
20. Ivanov, Y.F.; Konovalov, S. V.; Kormyshev, V.E.; Gromov, V.E.; Teresov, A.D.; Semina, O.A. Structure and Properties of Hardox 450 Steel with Arc Welded Coatings. *AIP Conf Proc* **2017**, *1909*, 1–6, doi:10.1063/1.5013754.
21. Zuo, Z.; Haowei, M.; Yarigarravesh, M.; Assari, A.H.; Tayyebi, M.; Tayebi, M.; Hamawandi, B. Microstructure, Fractography, and Mechanical Properties of Hardox 500 Steel TIG-Welded Joints by Using Different Filler Weld Wires. *Materials* **2022**, *15*, 4–6, doi:10.3390/ma15228196.
22. Akbar, R.; Awali, J.; Stasiyanur, F.; Lubis, M.P.D. Analysis of the Effect of Variations in Welding Current of the Combination of SMAW & FCAW Using Double V Groove on Tensile Strength, Impact and Microstructure in ASTM A36 Steel Weld Metal Area. *SPECTA Journal of Technology* **2023**, *7*, 434–442, doi:10.35718/specta.v7i1.704.
23. Özturan, A.B.; İrsel, G.; Güzey, B.N. Study of the Microstructure and Mechanical Property Relationships of Gas Metal Arc Welded Dissimilar Hardox 450 and S355J2C+N Steel Joints. *Materials Science and Engineering: A* **2022**, *856*, doi:10.1016/j.msea.2022.143486.
24. Wang, Z.; Wu, X.; Liu, D.; Zuo, X. Correlation Between Microstructure and Fracture Behavior in Thick HARDOX 450 Wear-Resistant Steel with TiN Inclusions. *Front Mater* **2021**, *8*, 691551, doi:10.3389/fmats.2021.691551.
25. Sun, J.; Jiang, T.; Liu, H.; Guo, S.; Liu, Y. Enhancement of Impact Toughness by Delamination Fracture in a Low-Alloy High-Strength Steel with Al Alloying. *Metallurgical and Materials Transactions A* **2016**, *47*, 5985–5993, doi:10.1007/s11661-016-3707-0.